

dr hab. inż. Maciej Major, prof. PCz.^{1*)}

ORCID: 0000-0001-5114-7932

dr inż. Jarosław Kalinowski¹⁾

ORCID: 0000-0001-8922-4788

dr inż. Mariusz Kosin¹⁾

ORCID: 0000-0003-2683-7784

The use of 3D printing technology to strengthen bendable cold-formed C-type profiles

Wykorzystanie technologii druku 3D do wzmocnienia zginanych zimnogiętych profili typu C

DOI: 10.15199/33.2023.10.05

Abstract. The article presents the use of 3D printing technology to strengthen cold-formed C-type steel profiles. The subject of the analysis were cold-formed steel beams stiffened in the middle of the span with elements made in 3D printing technology. The paper presents experimental and numerical results of three-point bending. Numerical calculations were carried out in the non-linear range of the material and taking into account large displacements. The analysis confirmed the increase in stiffness of the models subjected to three-point bending with the use of a stiffener made in the incremental printing technology with the use of ABS filament.

Keywords: 3D printing; cold-formed profiles; bending; numerical calculations.

Streszczenie. Artykuł przedstawia wykorzystanie technologii druku 3D do wzmocnienia stalowych profili zimnogiętych typu C. Przedmiotem analizy były zimnogięte belki stalowe usztywnione w połowie rozpiętości elementami wykonanymi w technologii druku 3D. Zaprezentowano wyniki doświadczalno-numeryczne trójpunktowego zginania. Obliczenia numeryczne przeprowadzono, uwzględniając nieliniowość materiału z uwzględnieniem dużych przemieszczeń. Analiza potwierdziła zwiększenie sztywności modeli poddanych trójpunktowemu zginaniu z wykorzystaniem usztywnienia wykonanego w technologii druku 3D z użyciem filamentu ABS.

Słowa kluczowe: druk 3D; profile zimnogięte; zginanie; obliczenia numeryczne.

Steel structures made of cold-bent elements constitute a group of load-bearing structures characterized by good strength indicators in relation to their own weight [1]. However, cold-bent sections are susceptible to loss of global and local stability. One of the methods of protecting cold-formed elements against loss of stability is the use of profiles with a complex cross-sectional shape. However, there may be a need to strengthen elements made using light steel frame technology during the building's operation stage. For this purpose, the authors conduct, among others, research on a solution to increase the load-bearing capacity and stiffness of cold-bent profiles in buildings.

The process of profiling cold-bent elements enables, among others: shaping the walls of cross-sections with edge and intermediate stiffening.

Thanks to additional stiffeners, the load-bearing capacity of the section walls is increased, and consequently also of the entire cross-section [2]. Thin-walled open-section bars can be stiffened along the entire length of the profile or at points. In practice, there are many known methods of stiffening thin-walled profiles with lacing, diaphragms or grating. This type of stiffeners limits the de-planation of the bar cross-section, reducing internal forces and displacements [3]. The numerical approach to modeling thin-walled elements is included in Annex C to PN EN 1993-1-5 [4] and [1]. The authors of [5] presented a sensitivity analysis of the behavior of a thin-walled I-section bar due to changes in the parameters of the battens.

The article presents an assessment of the possibility of using elements stiffening cold-bent steel profiles made using 3D printing technology – three-dimensional elements are created on the basis of a three-dimensional model by hardening the material (filament), layer

by layer [6, 7]. The proposed stiffening is composed of three elements which, when inserted into a cold-bent steel profile, wedge together to form one whole. The invention was submitted to the Patent Office in Poland under number P. 423102 [8] on February 11, 2020, and it was granted patent protection on April 30, 2020. The proposed solution was also the topic [9], where the impact of stiffening on flexural-torsional loads in the range of linear work of materials was presented.

Using the discussed technology, an experimental and numerical analysis of three-point bending of cold-bent beams was carried out, taking into account material nonlinearity. The mechanical properties of the steel used in cold-bent profiles and the filament used to make stiffening elements were also determined. The 3D printing method is not yet widely used in construction and requires many analyzes related to its effectiveness. The results presented in the article provide information necessary in the

¹⁾ Politechnika Częstochowska, Wydział Budownictwa

^{*)} Correspondence address: maciej.major@pcz.pl

process of designing new solutions, possibilities of their optimization and practical use.

Subject, scope and purpose of research

The tests were carried out on cold-bent steel C-section profiles stiffened at mid-span. **An original solution made of ABS filament using additive technology (3D printing) was used for stiffening.** The scope of the research included experimental and numerical three-point bending of beams in two configurations: a beam without stiffening and a beam stiffened with 3D printed elements. In the case of the adopted configurations, three three-point bending tests were performed. The tests were carried out in the full load range, up to the failure of the beams. Additionally, the mechanical properties of the profile material and 3D stiffener structure were determined, and the obtained results were used to perform numerical analysis.

The aim of the research was to compare the effectiveness of the presented solutions. Additionally, experimental research was used to numerically validate the adopted models.

Experimental research

Experimental tests were carried out in the **Laboratory of the Department of Civil Engineering of the Częstochowa University of Technology**. In order to determine the strength parameters, a tensile test was carried out in accordance with the PN-EN ISO 6892-1:2020-05 standard [10] in the case of steel samples and the PN-EN ISO 527-2:2012 standard – samples made using 3D printing technology [11]. Figure 1 shows the dimensions of the elements used in the tensile test. The filling density for samples made using ABS filament was 100%.

To test the mechanical properties of the samples, a testing machine with a maximum load of 50 kN and an increase in the traverse displacement of 0.03 mm/s was used. The three-point bending test was carried out using a testing machine with a maximum load of 100 kN. Due to the limitations of the testing machine, the length of the bent

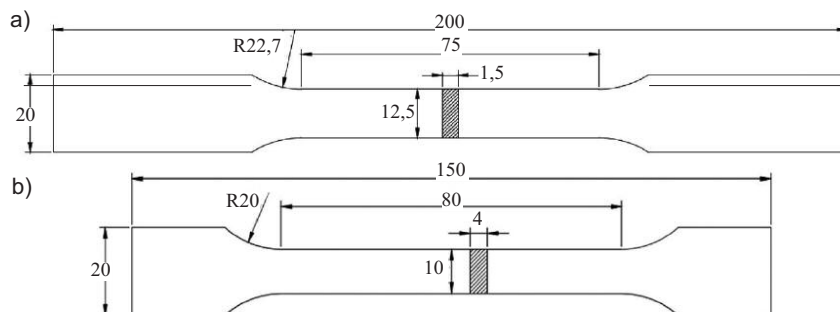


Fig. 1. Strength test samples: a) steel; b) made of ABS filament; dimensions are in mm
Rys. 1. Próbkki do badań wytrzymałościowych: a) stalowa; b) z filamentu ABS; wymiary podano w mm

beam was 830 mm and the distance between the supports was 560 mm. The increment of the traverse displacement was 0.5 mm/s.

Cold-bent profiles are made of cold- or hot-rolled galvanized steel sheet. In the EN 1993-1-3 Eurocode standard [12], steel grades and their nominal values are given. The analysis carried out considered a cold-bent C-shaped profile with the dimensions given in Table 1.

Table 1. Nominal and actual dimensions of the tested C90 profiles

Tabela 1. Wymiary nominalne i rzeczywiste badanych profili C90

	Cross-section dimensions of the C90 profile	Dimensions [mm]	
		nominal	actual
a		90	90
b		38	37,8
s		18	17,5
t		1.5	1,5
r		3	3

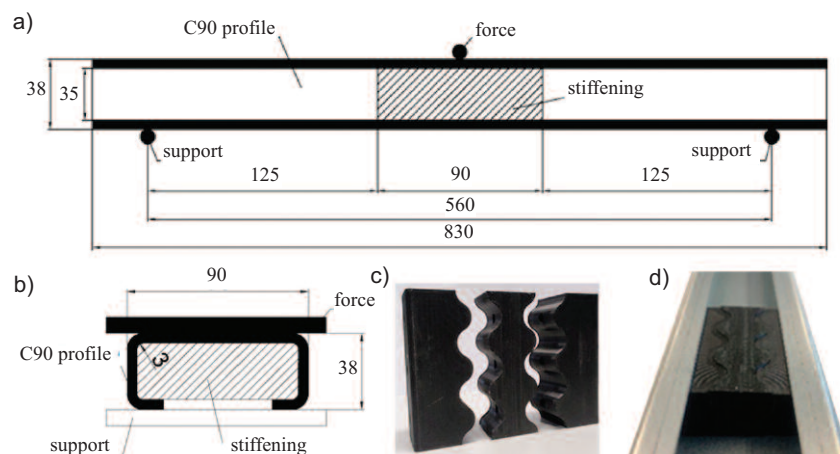


Fig. 2. Tested beams: a) longitudinal section of the beam; b) cross-section of the beam – dimensions in mm; c) the stiffening element; d) the stiffening element embedded in the profile

Rys. 2. Badane belki: a) przekrój podłużny belki; b) przekrój poprzeczny belki – wymiary w mm; c) element usztywniający; d) element usztywniający osadzony w profilu

The numerical model of three-point bending was built in accordance with the actual dimensions of the profile given in Table 1 and the diagram shown in Figure 2. The adopted numerical model was based on surface and solid elements [14, 15]. The thin-walled profiles were modeled using 4-node shell elements of the Shell 181 type, while the stiffening elements, the loading element and the supports were modeled as Solid 187 solid elements (10 nodes) [14, 16]. A nonlinear isotropic material was assumed for the calculations both in the case of profiles and stiffening elements. The experimentally determined strength characteristics of the stress-strain curve were converted into a real curve as a result of conversion using logarithmic equations and used for numerical calculations [17]. The basic material data used in the numerical analysis is presented in Table 2. The most unfavorable results obtained from the tensile strength test of steel and ABS filament were also taken into account for the analysis.

Table 2. Basic technical parameters of materials used to the numerical model
Tabela 2. Podstawowe parametry techniczne materiałów przyjętych w modelu numerycznym

Material	Young's modulus [MPa]	Poisson's ration	Yield strength [MPa]
Steel	200,65	0,3	381,08
ABS filament	1247,9	0,38	20,97

The analyzed numerical models take into account contact between frictional elements. Frictional contact allows the elements to separate and slide against each other [13, 14]. A friction coefficient of 0.17 was assumed in the case of profile-support contact and 0.35 - between the profile and the stiffening insert and in the case of the elements of the stiffening insert itself, the so-called profile stiffening. A finite element mesh was used to discretize the model, assuming the dimensions of each element were 3 mm. The adopted discretization method ensured sufficiently accurate observation of the strain and stress states occurring in the analyzed model. The boundary

conditions were defined in a way that allows for three-point bending by locking the support sections in the plane (Figure 3). The model was loaded due to the non-linear relationship

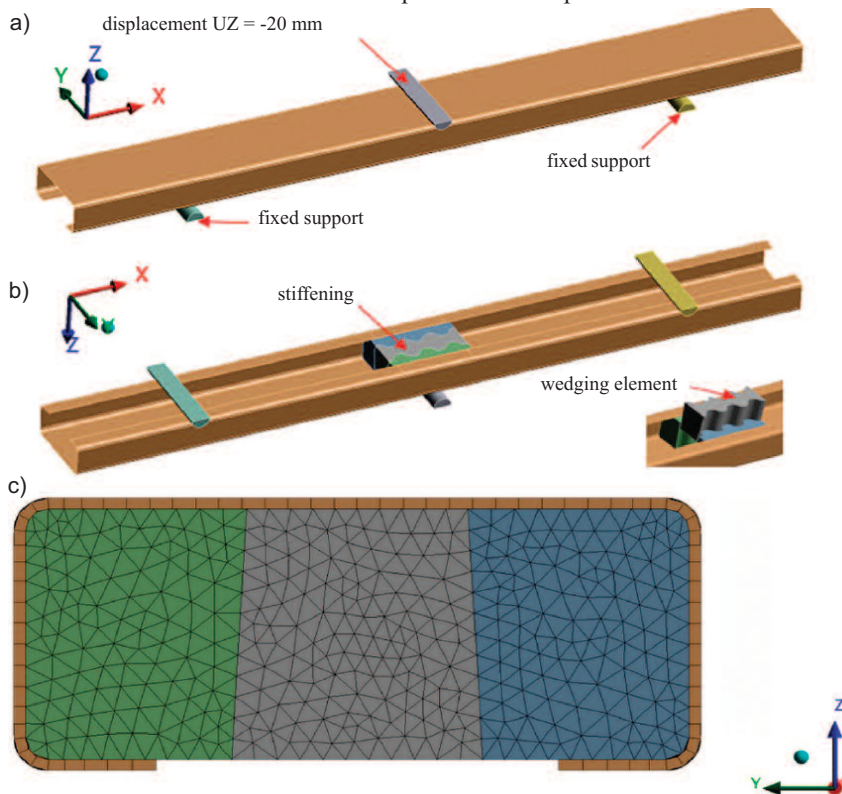


Fig. 3. The numerical model: a) boundary conditions and load; b) considered stiffening in the form of an insert made in 3D printing technology; c) mesh of finite elements

Rys. 3. Model numeryczny: a) warunki brzegowe i obciążenie; b) rozpatrywane usztywnienie w postaci wkładki wykonanej w technologii druku 3D; c) siatka elementów skończonych

between load and displacement by forcing a displacement of $U_Z = -20$ mm (Figure 3a).

Results analysis

The purpose of the static tensile test was to obtain information on the basic mechanical properties of steel and filament. The obtained results were used to create real curves used in numerical calculations. Figure 4 shows the graphs obtained during the static tensile test of samples made of steel and ABS filament. Based on the static tensile test, the basic parameters of the materials were determined, which were used, among others, in numerical analysis (Table 2). Figure 5 shows the actual curves used to describe material models in numerical analysis, in the case of the most unfavorable results obtained in the tensile test.

The assessment of the degree of reinforcement of steel profiles with stiffening elements was carried out on the basis of the force-displacement relationship for the transverse central

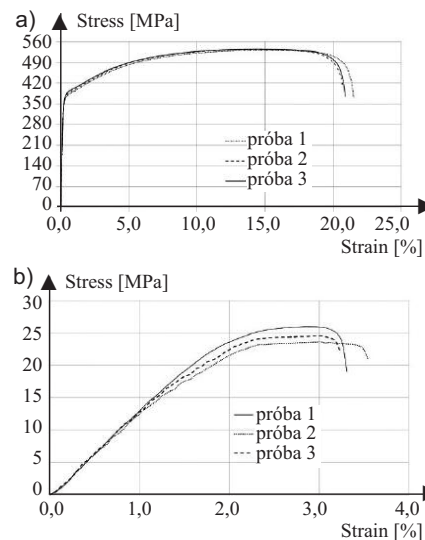


Fig. 4. Relationships between stress and strain obtained from the tensile test of the samples: a) steel; b) made of ABS filament
Rys. 4. Zależności między naprężeniem a odkształceniem uzyskane z próby rozciągania próbek: a) stalowych; b) z filamentu ABS

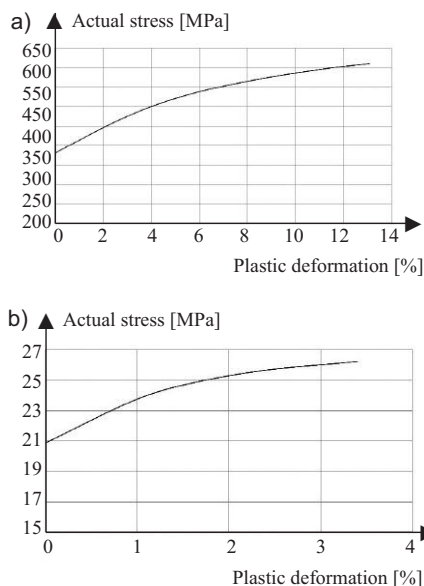


Fig. 5. Real curves used to description of materials models adopted for numerical analysis: a) steel; b) filament

Rys. 5. Krzywe rzeczywiste przyjęte do opisu modeli materiałów użytych do analizy numerycznej: a) stali; b) filamentu

section of the analyzed beams. Figure 6 shows the course of deformation of the steel profile web of experimentally and numerically tested thin-walled cold-bent beams. The obtained numerical results are qualitatively consistent with the experimental results (Figure 6). In the area of linear-elastic behavior, the beam deformations determined numerically are consistent with the deformations obtained experimentally. Discrepancies between the numerical and experimental results are observed in the elastic-plastic phase of the beam operation, after the profile has plasticized.

The beam deformations shown in Figure 7 correspond to the full load range. In the case of beams without stiffening, there was a local loss of stability at the point where the load was applied (Figure 7a). The deformation of the web of the stiffened beam shown in Figure 7b compared to the unstiffened beam differs in the number and location of zones where permanent deformations occur.

The performed numerical analysis, taking into account the nonlinearity of the material, enabled the assessment of the degree of deformation of the tested profiles. Based on the maps of displacements

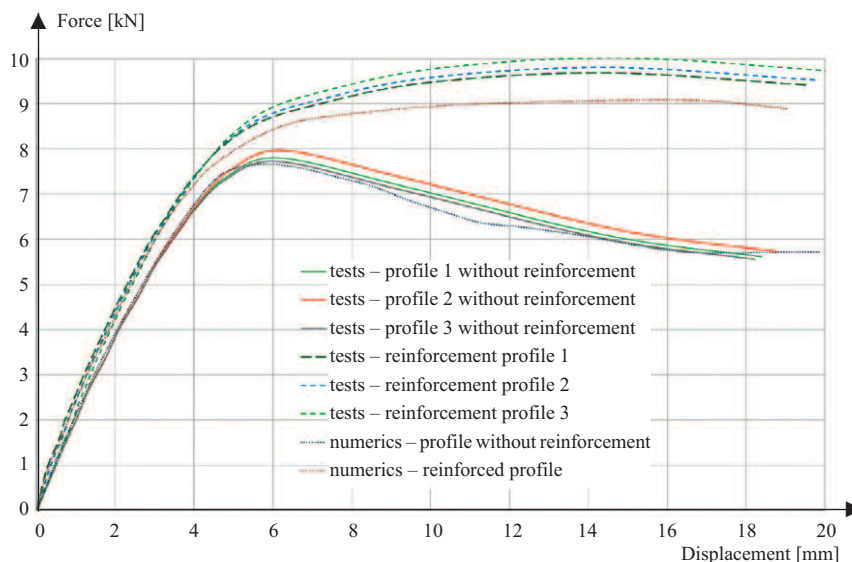


Fig. 6. Comparison of force-displacement curves, of experimental beams with numerical models

Rys. 6. Porównanie krzywych siła – przemieszczenie belek z badań doświadczalnych z modelami numerycznymi



Fig. 7. The tested cold-formed steel beams: a) without stiffening; b) with stiffening in the form of an insert made in 3D printing technology

Rys. 7. Badane stalowe belki zimnogięte: a) bez usztywnienia; b) z usztywnieniem w postaci wkładki wykonanej w technologii druku 3D

ments and reduced stresses of the numerical model, the most stressed places can be observed (Figures 8 and 9).

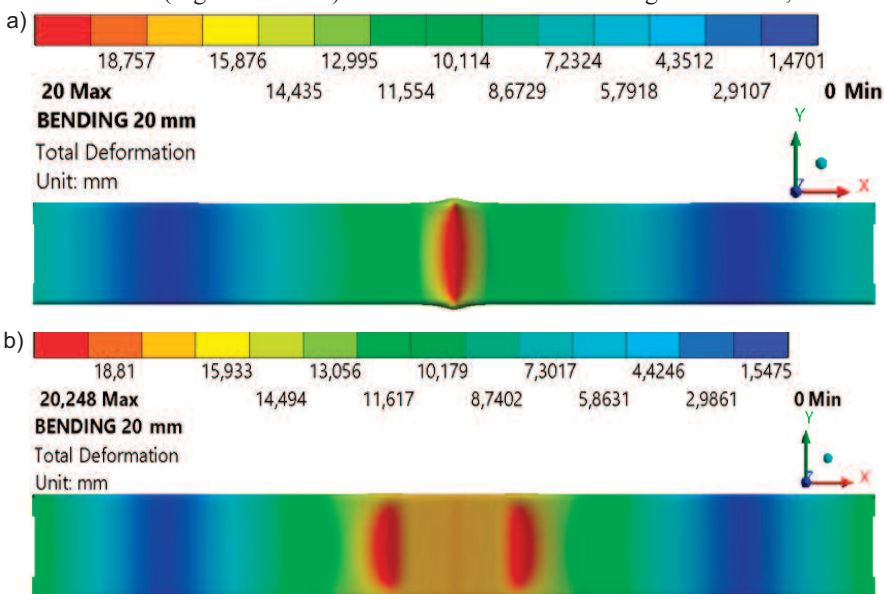


Fig. 8. The map of displacements for the profiles: a) unstiffened; b) stiffened

Rys. 8. Mapy przemieszczeń w przypadku profili: a) nieusztywnionych; b) usztywnionych

The results of numerical calculations of the adopted configurations, as in the experimental tests, differ in the number and place of local loss of plastic stability (Figures 8 and 9). In both models considered, the loss of stability took the form of local deformation of the web and flanges of the C-profile, characterized by a specific number of waves along its length. In the case of an unstiffened profile, the obtained form of stability loss was characterized by the occurrence of a single wave on the web and flanges. However, in a stiff-

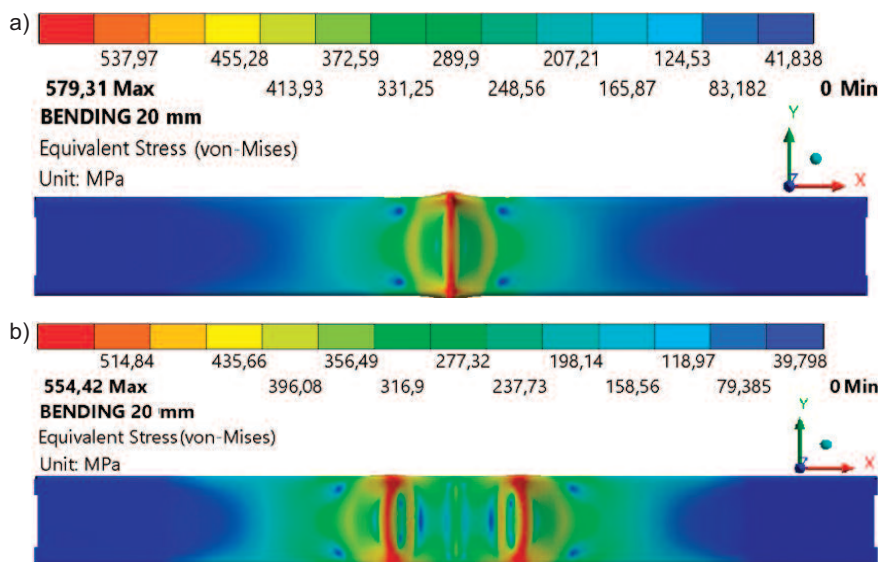


Fig. 9. The map of reduced stresses for the profiles: a) unstiffened; b) stiffened

Rys. 9. Mapa naprężeń zredukowanych w przypadku profili: a) nieusztywnionych; b) usztywnionych

fined profile, additional local deformations appear on the flange and web within the stiffener location. The numerically obtained images of damaged beams confirm the results obtained in experimental tests.

Conclusions

The effectiveness of stiffening cold-bent C-section profiles with elements made using 3D printing technology was assessed. The stiffened cold-bent C-profiles were subjected to three-point bending and compared with the behavior of beams without stiffening. Experimental research was supported by numerical calculations, which provided information of practical importance, necessary in the process of creating new solutions for 3D structures using 3D printing technology.

The three-point bending analysis carried out regarding the assessment of load transfer efficiency in the case of unstiffened and stiffened beams shows the influence of the 3D stiffening elements used on the strain of the profiles in the entire range of their operation. In the analyzed cases, the difference between the average ultimate load obtained for unstiffened beams is 20% smaller compared to stiffened beams. In the elastic limit for both beam configurations, sample calculations were made for a loading force of

6 kN. The average displacement values for the three beams without and with reinforcement were 3.44 and 2.956 mm, respectively. After applying the reinforcement, the stiffness of the beam increased by approximately 16%.

The behavior of the numerical beam models described by the force-displacement relationship in the middle of the span of the tested elements indicates qualitative agreement with the experimental results over the entire load range. Satisfactory agreement is observed in the presented real images of damaged beams in correlation with numerical tests. Inaccuracies in the area of buckling on the profile web can be observed in the case of stiffened profiles (Figures 7b, 8 and 9). This may be related to the asymmetrical arrangement of the stiffener in the tested profile and the place of force application.

It should be borne in mind that difficulties in obtaining a numerical solution consistent with the experimental one may also result from the adopted minimum step of displacement increment. The presented issue of using 3D printing to improve the operation of elements and structures made using light steel frame technology includes, among others: aspects related to determining the mechanical properties of designed 3D structures [2].

Literatura

- [1] Dubina D, Ungureanu V, Landolfo R. Design of cold-formed steel structures. The European Convention for Constructional Steelwork Brussels. Hancock G. J., 2003. Cold-formed steel structures. Journal of Constructional Steel Research. 2012; 118: 59 – 73.
- [2] Urbańska-Galewska E, Kowalski D. Zastosowanie lekkich konstrukcji stalowych do renowacji, rozbudowy i remontów obiektów budowlanych, XXIII Ogólnopolska Konferencja, Szczyrk 2008.
- [3] Gosowski B. Zginanie i skręcanie cienkościennych elementów konstrukcji metalowych, Oficyna Wydawnicza Politechniki Wrocławskiej, Wrocław 2015.
- [4] PN-EN 1993-1-5 2008, Eurokod 3 – Projektowanie konstrukcji stalowych – Część 1-5: Blachownice.
- [5] Szymczak Cz., Kreja I. Analiza wrażliwości dwuteowego pręta cienkościennego ze względu na zmiany parametrów przewiązek, Inżynieria i Budownictwo. 2003; 593.
- [6] Major M, Kalinowski J, Kosiń M. Wytrzymałość na rozciąganie elementów drukowanych z materiałów ABS, PA6+CF15, PA12+CF15. Materiały Budowlane. 2022; DOI: 10.15199/33.2022.10.21.
- [7] Ngo TD, Kashani A, Imbalzano G, Nguyen KTQ, Hui D. Additive manufacturing (3D printing): A review of materials, methods, applications and challenges. Composites Part B. 2018; 143.
- [8] Major M, Kalinowski J, Kosiń M. Wkładka usztywniająca, zwłaszcza cienkościennych profili typu C, Politechnika Częstochowska, 234844, Wiadomości Urzędu Patentowego 04/2020.
- [9] Kosiń M, Major I, Major M, Kalinowski J. Model Tests of Bending and Torsional Deformations of Thin-Walled Profiles Stiffened with Elements Made in 3D Printing Technology, Case Studies in Construction Materials. 2020; DOI: 10.1016/j.cscm.2020.e00401.
- [10] PN-EN ISO 6892-1:2020-05, Metale – Próba rozciągania – Część 1: Metoda badania w temperaturze pokojowej.
- [11] PN-EN ISO 527-2:2012. Tworzywa sztuczne – Oznaczanie właściwości mechanicznych przy statycznym rozciąganiu – Część 2: Warunki badań tworzyw sztucznych przeznaczonych do różnych technik formowania. 2013.
- [12] PN-EN 1993-1-3 2008, Eurokod 3, Projektowanie konstrukcji stalowych – Część 1-3: Reguły ogólne – Reguły uzupełniające dla konstrukcji z kształtowników i blach profilowanych na zimno.
- [13] Huei-Huang Lee Finite Element Simulations with Ansys Workbench 13 Schroft Development Corporation 2011.
- [14] Ansys – Workbench v. 18.1 system documentation, Ansys, Inc. Southpointe 275 Technology Drive Canonsburg, PA 15317.
- [15] Krześciński G, Zagrajek T, Marek P, Borkowski P. Metoda elementów skończonych w mechanice materiałów i konstrukcji. Rozwiązywanie zagadnień za pomocą systemu Ansys. Oficyna Wydawnicza Politechniki Warszawskiej Warszawa. 2015.
- [16] Łączek S. Modelowanie i analiza konstrukcji w systemie MES ANSYS v. 11, Wydawnictwo PK, Kraków 2011, ISBN 978-83-7242-584-3.
- [17] Petrik A, Aroch R. Usage of true stress-strain curve for FE simulation and the influencing parameters, IOP Conf. Materials Science and Engineering. 2019; 566.

Accepted for publications: 16.08.2023 r.